2022

Green synthesis of silver nanoparticles from Heteropyxis natalensis leaf extract and their potential antibacterial efficacy

D. Meer, S

10.2306/scienceasia1513-1874.2022.039
ScienceAsia
Science Society of Thailand

RESEARCH ARTICLE
doi: 10.2306/scienceasia1513-1874.2022.039

ScienceAsia 48 (2022): **196–201**

Green synthesis of silver nanoparticles from *Heteropyxis natalensis* leaf extract and their potential antibacterial efficacy

Saiyuri D. Meer[a], Yougasphree Naidoo[a], Yaser H. Dewir[b,*], Johnson Lin[a], Hail Z. Rihan[c,d]

[a] School of Life Sciences, University of KwaZulu-Natal, Westville Campus, Durban 4000 South Africa
[b] Plant Production Department, College of Food and Agriculture Sciences, King Saud University, Riyadh 11451 Saudi Arabia
[c] University of Plymouth, School of Biological Sciences, Faculty of Science and Environment, United Kingdom
[d] Phytome Life Sciences, Launceston, PL15 7AB, United Kingdom

[*]Corresponding author, e-mail: ydewir@ksu.edu.sa

Received 21 Jun 2021
Accepted 30 Nov 2021

ABSTRACT: Silver nanoparticles (AgNPs) are sought after by many industries including food industries, heavy metal sensing, pharmaceutical, and textile. The present study reports on the biosynthesis of silver nanoparticles (AgNPs) and theirs antibacterial activity using a methanolic leaf extract of *Heteropyxis natalensis*, a native South African medicinal tree. The synthesised particles were characterised by ultraviolet visible spectroscopy (UV-vis), energy dispersive X-ray spectroscopy (EDX), high resolution transmission electron microscopy (HRTEM), and Fourier transform infrared spectroscopy (FTIR). A colour change of the reaction solution from yellow to brown preliminarily confirmed the presence of AgNPs, and a single absorbance peak at 422 nm, using UV-vis spectroscopy, was the indicative of AgNPs. While EDX revealed the presence of elemental silver in the sample, HRTEM identified spherical AgNPs ranging from 5–60 nm. Hydroxyls, alkynes, alkenes, alkanes, esters, and alkyl halides as possible capping agents of silver ions (Ag^+) into AgNPs were identified by FTIR. In addition, AgNPs exhibited antibacterial efficacy against 5 strains of pathogenic bacteria: *Escherichia coli*, *Staphylococcus aureus*, methicillin-resistant *Staphylococcus aureus*, *Pseudomonas aeruginosa*, and *Bacillus subtilis*. The results obtained in this study could potentially benefit future research in nanomedical-driven fields.

KEYWORDS: AgNPs, silver, nanoparticles, antibacterial efficacy, characterisation

INTRODUCTION

Nanotechnology is a research field that is currently evolving [1] at an exponential rate with the aim of revolutionising the medical world [2]. This field of study involves the synthesis, the development, and the manipulation of nanomaterials ranging from 0–100 nm [3, 4]. Over the years, nanotechnology has been introduced into various medical applications; for example, gene therapy, cancer treatment, and drug delivery [3, 5]. Metals such as copper, zinc, gold, titanium and silver are used to produce nanoparticles [1, 6, 7]. The synthesis of metal nanoparticles has gained significant importance due to the particle's unique optical, electronic, magnetic, chemical, and antimicrobial characteristics [8]. As a result, metallic nanoparticles present advantageous opportunities in various industries: medical, pharmaceutical, and textile industries as well as in heavy metal sensing [6, 9]. Silver (Ag) is considered an ideal metal for the synthesis of nanoparticles [8], and AgNPs are at the forefront of nanotechnology sought after for several applications due to their unique structural properties [10, 11]. They have been successfully exploited in pathology, medicine, textile, food, and pharmaceutical industries [12, 13]. The synthesis of nanoparticles can occur through the use of chemical, physical, biological, and hybrid methods [5]. However, chemical and physical methods are considered toxic and non-ecofriendly [11]. Scientists are currently relying on safer alternatives such as "green synthesis", which is defined as using non-toxic, environmentally friendly biological materials in the synthesis method [10, 11, 14]. This approach brings nanotechnology and plant biotechnology together resulting in a system that is risk-free with superior quality suitable for biomedical applications [4, 6]. Plants have previously been used to synthesize AgNPs as they are inexpensive, efficient, safe, and environmentally friendly [15]; and, moreover, phytochemicals present in plant extracts serve as perfect reducing and capping agents during the synthesis [13]. Medicinal plants are known for their antimicrobial properties against bacteria, fungi, and viruses [15]. AgNPs were reported to be efficient antibacterial agents [1, 10]; hence, antimicrobial researches have focused on their antimicrobial potentials.

Heteropyxis natalensis (Myrtaceae) is a small, deciduous tree inhabiting in evergreen forests and bushveld regions ranging from KwaZulu-Natal to Limpopo Provinces in South Africa [16, 17]. The leaves, bark, and roots of *H. natalensis* have previously been reported to exhibit medicinal and antimicrobial properties [16]. Venda and Zulu communities utilise *H. natalensis* to treat several ailments such as respiratory disorders, nosebleeds, and gingivitis [17–19]. To

the authors' knowledge, there are no reports available on silver nanosynthesis on this species. Therefore, this study aimed to examine the synthesis, characterization, and the potential antibacterial efficacy of AgNPs using crude methanolic leaf extract of *H. natalensis*.

MATERIALS AND METHODS

Preparation of crude leaf extract

Fresh and healthy leaves of *H. natalensis* were collected from the University of KwaZulu-Natal, Westville Campus (29°49′01.0″ S 30°56′51.2″ E) in Durban, South Africa. The leaves were cleaned using double distilled water and air dried at 24 °C for 6 weeks. A voucher specimen was deposited in the Ward Herbarium at the University of KwaZulu-Natal. The dried leaves were ground into a fine powder using a domestic spice mill (Kenwood Ltd, Havant, UK), and the crude extract was prepared using a soxhlet apparatus. Powdered leaf material (±2.5 g) was added to 50 ml of methanol (HPLC grade) in a round bottom flask. The powder and solvent mixture was boiled for 2 h followed by a 1 h session. Thereafter, the mixture was filtered using Whatman filter paper No. 1, and the methanolic extract (the filtrate) was stored in a mason jar at 24 °C in a dark room.

Biosynthesis of silver nanoparticles

The biosynthesis of AgNPs was conducted according to a method described by [20] with a few modifications. Methanolic extract (1 ml) was added to 19 ml of a 1 mM aqueous silver nitrate ($AgNO_3$) solution. The $AgNO_3$ and methanolic extract solution was mixed in a conical flask and incubated in a water bath at 60 °C for 30 min. A colour change the solution from yellow to brown indicated the formation of AgNPs. Thereafter, the solution was centrifuged at 16 000 rpm for 5 min using an Eppendorf Centrifuge 5415R (Merck, Johannesburg, South Africa). After removing the supernatant, deionised water ($_{di}H_2O$) was added to the Eppendorf tube and centrifuged. The centrifugation process was repeated thrice. The resultant pellet was then suspended in 10 ml of $_{di}H_2O$, vortexed, and further used for characterisation.

Characterisation of AgNPs

Ultraviolet visible spectroscopy (UV-vis)

The presence of AgNPs was confirmed by UV-vis spectroscopy. The absorbance spectrum was recorded using a UV-1800 Shimadzu spectrophotometer (Tokyo, Japan) at an absorbance wavelength range of 300–600 nm, and $_{di}H_2O$ was used as a blank.

Energy dispersive X-Ray spectroscopy (EDX)

A drop of synthesised AgNPs was placed directly onto an aluminium stub and was left to dry for 24 h. The stub was then sputter coated in a Polaron SC500 Sputtercoater. EDX microanalysis was conducted using an Ultra Plus Field Emission Gun Scanning Electron microscope (FEGSEM) (Carl Zeiss, Munich, Germany) and AzTec Analysis Software (Oxford Instruments, High Wycombe, UK) to determine the presence of elemental silver in the sample.

High resolution transmission electron microscopy (HRTEM)

A drop of sonicated synthesised AgNPs was placed on a copper grid and left to dry for 20 min. The overall micromorphology (shape and size) of AgNPs was observed using an HRTEM JEOL 2100, and the particle size was determined using iTEM software (Soft Imaging System GmBH, MÃijnster, Germany).

Fourier transform infrared spectroscopy (FTIR)

The capping and reducing agents of AgNPs were identified using FTIR. The FTIR measurements were conducted using a Perkin Elmer spectrum 100 spectrophotometer (MA, USA) at a wavelength of 4000–400 cm^{-1}.

Antibacterial activity

Preliminary screening of antibacterial activity of AgNPs was determined using the agar well diffusion method described by [21] against two strains of gram-negative bacteria: *Escherichia coli* (ATCC 25218) and *Pseudomonas aeruginosa* (ATCC 27853), and three gram-positive bacterial strains: *Staphylococcus aureus* (ATCC 25923), methicillin-resistant *Staphylococcus aureus* (MRSA) (Clinical type), and *Bacillus subtilis*. The bacterial strains were grown for 18 h in Nutrient Broth (Biolab, Midrand, South Africa) in a 37 °C incubator on a shaker and were then standardised by measuring optical density using a UV-vis spectrophotometer (equivalent to 0.5 McFarland turbidity standard; OD 0.08–0.1 at λ 625 nm). The optical densities were further adjusted by dilution of the bacterial inoculum with sterile distilled water. The Tmlhe medium was prepared by mixing 38 g Mueller Hinton agar (MHA) in 1 l of $_{d}H_2O$, boiled for 1 min, and autoclaved at 121 °C for 20 min. After reaching room temperature (24 °C), the medium was carefully poured into sterile petri dishes and left to solidify under a sterile environment. Each bacterial strain was evenly swabbed onto the MHA plates and left to dry. Wells were aseptically punched using a sterile cork borer (5 mm in diameter). Thereafter, 90 µl of the AgNP stock solution (1 mg/ml) was pipetted into each well. The petri dishes were then transferred to incubators of various temperatures to allow the solution to diffuse through the medium, and inhibition zones were observed after 18 h.

Statistical analysis

All the experiments were conducted with three replicates. For antibacterial activity, the zone of inhibition was measured and presented as mean values and the statistical analysis was performed using a Student's *t*-test.

RESULTS AND DISCUSSION

Biosynthesis and characterization of AgNPs

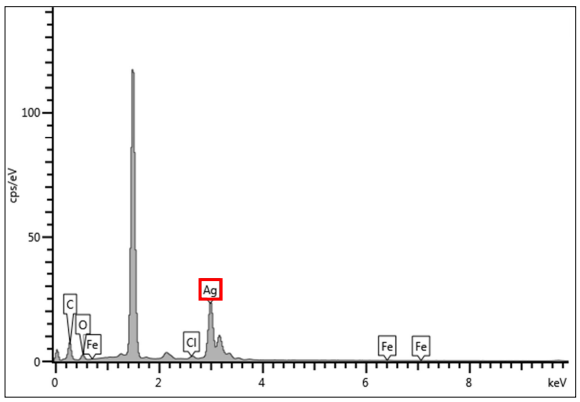

Fig. 1 EDX analysis of synthesized AgNPs from *H. natalensis* methanolic leaf extract.

In the present study, the formation of AgNPs was observed based on a gradual colour change in the reaction vessel from yellow to dark brown over 30 min. In general, the biosynthesis of AgNPs is often confirmed by a colour change of the reaction solution [22, 23] as a consequence of the surface plasmon resonance (SPR) [24, 25] indicative of the reduction of Ag^+. The reduction of Ag^+ may be attributed to the chemical components present in the leaf extract [20]. In addition, the synthesis of AgNPs was further confirmed by UV-vis spectroscopy which determined the progression of the reduction of Ag^+ [26]. A single absorbance peak was observed at 422 nm which was indicative of SPR of AgNPs [8]. Absorbance peaks observed between wavelengths of 410 and 450 nm may have been attributable to the presence of spherical nanoparticles [5, 27]. Similar absorbance peaks were observed in a study conducted on several myrtaceous species including *Xanthostemon chrysanthus* (424 nm) and *Callistemon lanceolatus* (420 nm) [15].

The elemental composition of synthesised AgNPs was investigated by EDX. In Fig. 1, the EDX spectrum revealed a peak at 3 keV displaying elemental silver (60.5%). Silver nanocrystals often have an optical absorption peak at 3 keV as a result of SPR [5]. This indicates the reduction of Ag^+ into elemental silver and authenticates the synthesis of AgNPs [5, 12, 14]. Additional elements present in the 0–0.5 keV range denoted the optical absorption of carbon (22.81%) and oxygen (16.03%) [26]; and a peak at 2.5 keV signified the absorption of chlorine (0.30%). The presence of these elements suggests that they have emanated from *H. natalensis* leaf extract and act as capping agents for AgNPs [15, 20, 26]. These results confirm previous findings wherein the EDX spectrum revealed the presence of elemental silver and additional elements after synthesizing AgNPs using *Eucalyptus oleosa* leaf extract [28].

Table 1 FTIR peak values, functional groups, and vibration types of AgNPs from *H. natalensis* methanolic leaf extract.

Absorption peak (cm^{-1})	Functional group	Type of vibration
3268.08	O—H	Stretch
2118.83	C≡C	Stretch
1638.42	C=C	Stretch
1374.95	C—H	Bending
1217.16	C—O	Stretch
1016.61	C—O	Stretch
575.93	C—Br	Stretch

The morphology and particle size distribution of synthesized AgNPs are shown in Fig. 2A and Fig. 2B, respectively. The structural morphology of synthesized particles appeared to be spherical in nature with an average size of 23.38 nm in diameter. The morphology of nanoparticles primarily relied on the reduction of the efficacy of the reducing agents present in the leaf extract [27]. The size of the particles was between 5–60 nm. However, many particles were observed to be in the 10–20 nm range which justifies the single absorbance peak at 422 nm. Variation of methods was used to identify and measure AgNPs with advantages and limitations to the individual techniques. Therefore, a combined approach is considered the most suited method to measure the particle size and to determine the particle shape [29]. AgNPs were well dispersed after sonication and displayed crystalline characteristics as shown by distinct lattice fringes (inset). The histogram in Fig. 2B indicates that the AgNPs were not uniform in size; however, the particles were below 100 nm making them suitable for the uses in textile, food, and medical fields [12]. The shape and size of AgNPs were similar to the particles synthesized in a study of several myrtaceous species [15].

The functional groups of AgNPs were detected using FTIR spectroscopy between a scan range of 4000–400 cm^{-1}. The functional groups that were identified in the sample are recorded in Table 1 in accordance with the absorption bands (peaks) in the FTIR spectrum shown in Fig. 3. Hydroxyls, alkynes, alkenes, alkanes, esters, and alkyl halides were identified in the sample. The presence of these functional groups indicated that they belonged to secondary metabolites such as alkaloids, terpenes, and phenolics [15] present in the leaf extract of *H. natalensis*. In addition, these functional groups were responsible for the reduction, stabilization, and capping of Ag^+ into AgNPs [5, 30]. Hydroxyl, alkene, alkane, and ester functional groups were also identified in the synthesized AgNPs of *Syzygium campanulatum* and *Eucalyptus citriodora* [15]. A broad hydroxyl peak (3270.82 cm^{-1}) was detected in the FTIR spectrum of *Eucalyptus corymbia* [31], and the

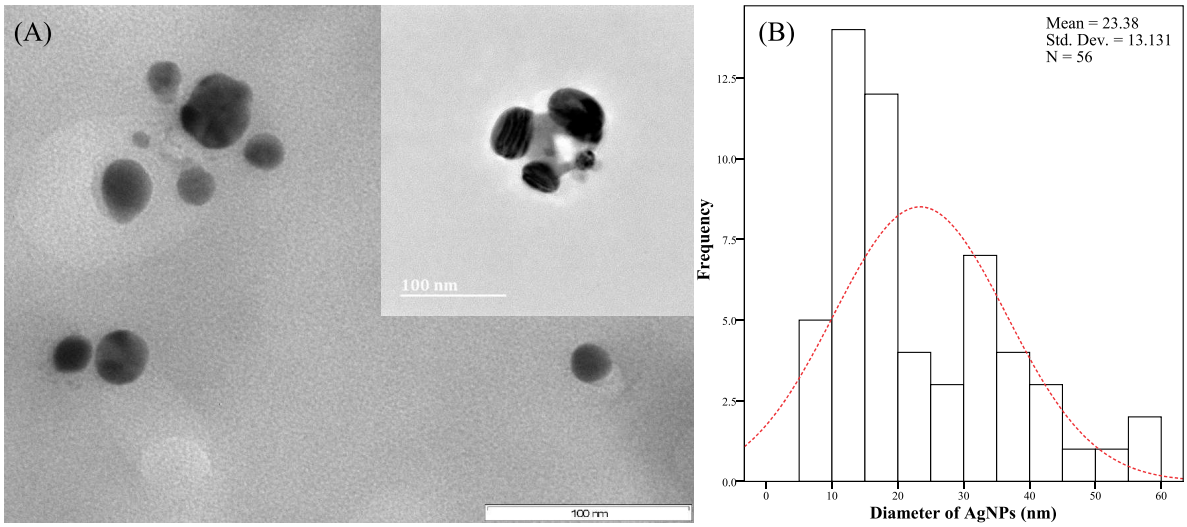

Fig. 2 Particle size distribution of AgNPs from *H. natalensis* methanolic leaf extract. (A) Electron micrograph of synthesized spherical AgNPs and distinct lattice fringes (inset). (B) Histogram representing the range of particles according to diameter size.

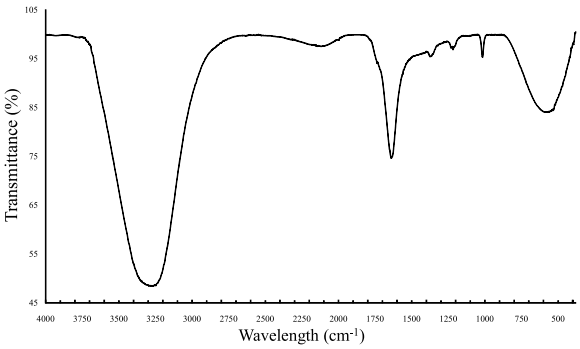

Fig. 3 FTIR spectrum of synthesized AgNPs from *H. natalensis* methanolic leaf extract.

Table 2 Preliminary screening of antibacterial activity of AgNPs from *H. natalensis* methanolic leaf extract.

Bacterial Strain	Zone of Inhibition (mm)[†]
Escherichia coli	8 b
Staphylococcus aureus	8 b
Pseudomonas aeruginosa	12 a
MRSA	8 b
Bacillus subtilis	7 b

[†] = inhibition zone including the cork borer (5 mm) diameter, MRSA = methicillin-resistant *Staphylococcus aureus*. Mean values followed by different letters are significantly different according Student's *t*-test.

peak was similar to the one identified in the current study (3268.08 cm^{-1}). This functional group was mainly involved in the synthesis of AgNPs in comparison to other functional groups in the sample [31].

Antibacterial activity

The antibacterial activity of synthesised AgNPs of *H. natalensis* is summarized in Table 2. The zones of inhibition varied against *E. coli*, *P. aeruginosa*, *S. aureus*, MRSA, and *B. subtilis*. Antibacterial activity against *P. aeruginosa* exhibited the highest zone of inhibition. *Pseudomonas aeruginosa* is an opportunistic bacterial strain [32] and often causes infections in immunocompromised postoperative patients suffering with cancer, burn wounds, and cystic fibrosis [33]. This bacterium also causes pneumonia, bacteremia, and gastrointestinal infections [33]. The smallest zone of inhibition was exhibited against *B. subtilis* indicating the least AgNPs sensitivity of the strain compared with the other strains used in this study. A small inhibition zone signifies the ability of bacteria to form endospores (resting stage) and enables the bacteria to remain viable and more resistant over time [34]. Furthermore, *P. aeruginosa* showed a large inhibition zone due to the presence of a cell wall consisting of an inner thin peptidoglycan layer and an outer liposaccharide layer. The thin cell wall increased the microbe's susceptibility to Ag^{+} as opposed to the Gram-positive bacteria [35].

Elemental silver has been used for centuries due to its reputable antimicrobial properties [36, 37], and synthesized AgNPs have been utilized in medicine, food storage, pharmaceuticals, and several environmental sectors [37]. The antibacterial effect is possibly attributed to the size of AgNPs [5]. As seen in Fig. 2B, the synthesized AgNPs were relatively small; however, their combined surface areas were large [5, 34] allowing the AgNPs to have a better contact and interaction with the bacteria [5]. As a result, the AgNPs attached

to the surface of the bacterial membrane resulting in its structural changes and eventually causing cell death [15, 38]. The results presented in Table 2 suggested that the synthesized AgNPs of *H. natalensis* can be used as effective antibacterial agents in the treatment of several ailments: gastrointestinal, skin, respiratory, and nosocomial. Besides, these results were consistent with the previous findings wherein myrtaceous AgNPs exhibited antibacterial activity against similar bacterial strains [30, 38].

CONCLUSION

An effective "green synthesis" of AgNPs using methanolic leaf extract of *H. natalensis* was demonstrated. A colour change of the reaction solution from yellow to brown as a result of SPR indicated the reduction of Ag^+ and the formation of AgNPs. Synthesized particles were below 100 nm and spherical in shape. Additionally, preliminary screening of AgNPs against various strains of bacteria highlighted the effectiveness of these particles as antibacterial agents. Lastly, the results obtained in this study could potentially benefit future researches in nanomedical-driven fields that utilize medicinal flora.

Acknowledgements: The authors acknowledge Researchers Supporting Project number (RSP-2021/375), King Saud University, Riyadh, Saudi Arabia. The authors extend their gratitude to Microscopy and Microanalysis Unit at the University of KwaZulu-Natal, and the National Research Foundation (NRF) for their support.

REFERENCES

1. Hasan S (2015) A review on nanoparticles: Their synthesis and types. *Res J Recent Sci* **4**, 1–3.
2. Saidi T (2018) Perceived risks and benefits of nanomedicine: A case study of an anti-tuberculosis drug. *Glob Health Innov* **1**, 1–7.
3. Mondal AK, Mondal S, Samanta S, Mallick S (2011) Synthesis of ecofriendly silver nanoparticle from plant latex used as an important taxonomic tool for phylogenetic interrelationship. *Adv Bio Res* **2**, 122–133.
4. Mohammed AE (2015) Green synthesis, antimicrobial and cytotoxic effects of silver nanoparticles mediated by *Eucalyptus camaldulensis* leaf extract. *Asian Pac J Trop Biomed* **5**, 382–386.
5. Jyoti K, Baunthiyal M, Singh A (2016) Characterization of silver nanoparticles synthesized using *Urtica dioica* Linn. leaves and their synergistic effects with antibiotics. *J Radiat Res Appl Sci* **9**, 217–227.
6. Parveen K, Banse V, Ledwani L (2016) Green synthesis of nanoparticles: Their advantages and disadvantages. *AIP Conf Proc* **1724**, ID 020048.
7. Lee KM, Yoong WC, Loke CF, Juan JC, Yusoff K, Mohtarrudin N, Lim TH (2021) Preparation of calcium alginate-encapsulated sulfur particles and their application in metal nanoparticle capture: A case study of silver nanoparticles. *ScienceAsia* **47**, 42–50.
8. Anandalakshmi K, Venugobal J, Ramasamy V (2016) Characterization of silver nanoparticles by green synthesis method using *Pedalium murex* leaf extract and their antibacterial activity. *Appl Nanosci* **6**, 399–408.
9. Siraja M, Shaha ZA, Ullahb S, Bibic H, Sulemana M, Ziaa A, Masooda T, Iqbala Z, et al (2020) Biosynthesized silver nanoparticles from shoot and seed extracts of *Asphodelus tenufolius* for heavy metal sensing. *ScienceAsia* **46**, 697–705.
10. Zargar M, Hamid AA, Bakar FA, Shamsudin MN, Shameli K, Jahanshiri F, Farahani F (2011) Green synthesis and antibacterial effect of silver nanoparticles using *Vitex negundo* L. *Molecules* **16**, 6667–6676.
11. Mishra PM, Pani KB (2017) Biomimetic synthesis of silver nanoparticles and evaluation of their catalytic activity towards degradation of methyl orange. *Mater Res Express* **4**, ID 11.
12. Mishra M, Chauhan P (2015) Nanosilver and its medical implications. *J Nanomed Res* **2**, ID 00039.
13. Bose D, Chatterjee S (2016) Biogenic synthesis of silver nanoparticles using guava (*Psidium guajava*) leaf extract and its antibacterial activity against *Pseudomonas aeruginosa*. *Appl Nanosci* **6**, 895–901.
14. Dubey M, Bhadauria S, Kushwah BS (2009) Green synthesis of nanosilver particles from extract of *Eucalyptus hybrida* (Safeda) leaf. *Dig J Nanomater Biostructers* **4**, 537–543.
15. Paosen S, Saising J, Septama AW, Voravuthikunchai SP (2017) Green synthesis of silver nanoparticles using plants from Myrtaceae family and characterization of their antibacterial activity. *Mater Lett* **209**, 201–206.
16. Van Vuuren SF, Viljoen AM, Özek T, Demirci B, Başer KHC (2007) Seasonal and geographical variation of *Heteropyxis natalensis* essential oil and the effect thereof on the antimicrobial activity. *S Afr J Bot* **73**, 441–448.
17. Adesanwo JK, Shode FO, Aiyelaagbe O, Oyede RT, Baijnath H (2009) Isolation and characterization of a new chalcone from the leaves of *Heteropyxis natalensis*. *Int J Med Med Sci* **1**, 23–32.
18. Van Vuuren S, Viljoen A (2008) Indigenous South African medicinal plants: part 10: *Heteropyxis natalensis* ('Lavender tree'): medicinal plants. *SA Pharm J* **75**, 46.
19. Henley-Smith CJ, Botha FS, Hussein AA, Nkomo M, Meyer D, Lall N (2018) Biological activities of *Heteropyxis natalensis* against micro-organisms involved in oral infections. *Front Pharmacol* **9**, ID 291.
20. Sudha A, Jeyakanthan J, Srinivasan P (2017) Green synthesis of silver nanoparticles using *Lippia nodiflora* aerial extract and evaluation of their antioxidant, antibacterial and cytotoxic effects. *Resour Effic Technol* **3**, 506–515.
21. Saif MMS, Al-Fakih AA, Hassan MAM (2017) Antibacterial activity of selected plant (Aqueous and methanolic) extracts against some pathogenic bacteria. *J Pharmacogn Phytochem* **6**, 1929–1935.
22. Dubey SP, Lahtinen M, Sillanpää M (2010) Green synthesis and characterizations of silver and gold nanoparticles using leaf extract of *Rosa rugosa*. *Colloids Surf A* **364**, 34–41.
23. Swamy MK, Sudipta KM, Jayanta K, Balasubramanya S (2015) The green synthesis, characterization, and evaluation of the biological activities of silver nanoparticles synthesized from *Leptadenia reticulata* leaf extract. *Appl Nanosci* **5**, 73–81.
24. Rout Y, Behera S, Ojha AK, Nayak PL (2012) Green synthesis of silver nanoparticles using *Ocimum sanctum*

(Tulashi) and study of their antibacterial and antifungal activities. *J Microbiol Antimicrob* **4**, 103–109.
25. Vijayakumar M, Priya K, Nancy FT, Noorlidah A, Ahmed ABA (2013) Biosynthesis, characterization and antibacterial effect of plant-mediated silver nanoparticles using *Artemisia nilagirica*. *Ind Crops Prod* **41**, 235–240.
26. Shaik MR, Khan M, Kuniyil M, Al-Warthan A, Alkhathlan HZ, Siddiqui MRH, Shaik JP, Ahamed A, et al (2018) Plant-extract-assisted green synthesis of silver nanoparticles using *Origanum vulgare* L. extract and their microbicidal activities. *Sustainability* **10**, ID 913.
27. Zaheer Z (2012) Silver nanoparticles to self-assembled films: green synthesis and characterization. *Colloids Surf B* **90**, 48–52.
28. Pourmortazavi SM, Taghdiri M, Makari V, Rahimi-Nasrabadi M (2014) Procedure optimization for green synthesis of silver nanoparticles by aqueous extract of *Eucalyptus oleosa*. *Spectrochim Acta Part A* **136**, 1249–1254.
29. Mourdikoudis S, Pallares RM, Thanh NTK (2018) Characterization techniques for nanoparticles: comparison and complementarity upon studying nanoparticle properties. *Nanoscale* **10**, 12871–12934.
30. Sekhar EC, Rao KK, Rao KMS, Alisha SB (2018) A simple biosynthesis of silver nanoparticles from *Syzygium cumini* stem bark aqueous extract and their spectrochemical and antimicrobial studies. *J Appl Pharm Sci* **8**, 073–079.
31. Sila JM, Kiio I, Mwaura FB, Michira I, Abongo D, Iwuoha E, Kamau GN (2014) Green synthesis of silver nanoparticles using *Eucalyptus corymbia* extract and antimicrobial applications. *Int J BioChemiPhysics* **22**, 21–30.
32. Singh K, Panghal M, Kadyan S, Chaudhary U, Yadav JP (2014) Antibacterial activity of synthesized silver nanoparticles from *Tinospora cordifolia* against multi drug resistant strains of *Pseudomonas aeruginosa* isolated from burn patients. *J Nanomed Nanotechnol* **5**, ID 1000192.
33. Salomoni R, Léo P, Montemor AF, Rinaldi BG, Rodrigues MFA (2017) Antibacterial effect of silver nanoparticles in *Pseudomonas aeruginosa*. *Nanotechnol Sci Appl* **10**, 115–121.
34. Liliwirianis N, Zain WZWM, Kassim J, Karim SA (2011) Antimicrobial activity of plant extracts against *Bacillus subtilis*, *Staphylococcus aureus* and *Escherichia coli*. *J Chem* **8**, 282–284.
35. Pazos-Ortiz E, Roque-Ruiz JH, Hinojos-Márquez EA, López-Esparza J, Donohué-Cornejo A, Cuevas-González JC, Espinosa-Cristóbal LF, Reyes-López SY (2017) Dose-dependent antimicrobial activity of silver nanoparticles on polycaprolactone fibers against Gram-positive and Gram-negative bacteria. *J Nanomater* **2017**, 4752314.
36. Dipankar C, Murugan S (2012) The green synthesis, characterization and evaluation of the biological activities of silver nanoparticles synthesized from *Iresine herbstii* leaf aqueous extracts. *Colloids Surf B* **98**, 112–119.
37. Ahmed S, Ahmad M, Swami BL, Ikram S (2016) Green synthesis of silver nanoparticles using *Azadirachta indica* aqueous leaf extract. *J Radiat Res Appl Sci* **9**, 1–7.
38. Yugandhar P, Savithramma N (2015) Biosynthesis, characterization and antimicrobial studies of green synthesized silver nanoparticles from fruit extract of *Syzygium alternifolium* (Wt.) Walp. an endemic, endangered medicinal tree taxon. *Appl Nanosci* **6**, 223–233.